# 9.1 Column buckling

| | |
|---|---|
| **REFERENCE** | Gerel et al.[1] |
| **ELEMENTS** | Bar elements, Shell elements, Solid elements |
| **MODEL FILENAME** | Buckling01_CASE1.fea<br>Buckling01_CASE2.fea<br>Buckling01_CASE3.fea<br>Buckling01_CASE4.fea |

Figure 9.1.1 shows a straight column model. Linear buckling analysis is carried out to determine the buckling modes and the corresponding critical loads of a column subjected to a vertical load. Four kinds of boundary conditions are considered. The lowest buckling modes are presented in Figure 9.1.2.

Figure 9.1.1
Column model

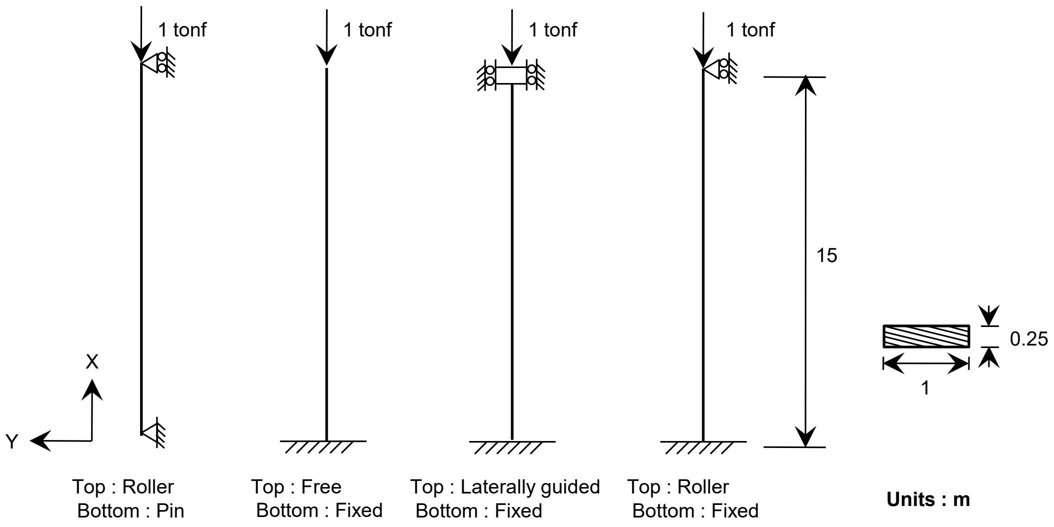


Figure 9.1.2
Buckling mode shapes

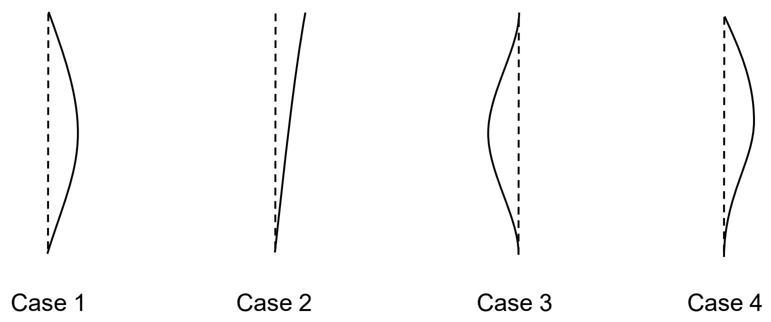


| | | |
|---|---|---|
| **Material data** | Young's modulus | 10,000 tonf/m$^2$ |
| **Section property** | Rectangular cross-section | 0.25 m × 1.0m |

*Table 9.1.1 Critical loads in tonf obtained using bar elements*

| Case number | | 1 | 2 | 3 | 4 |
|---|---|---|---|---|---|
| Reference | | 0.5712 | 0.1428 | 2.2846 | 1.1684 |
| Element type | Number of elements | | | | |
| Bar-2 | 15 | 0.5714 | 0.1428 | 2.2891 | 1.1695 |

*Table 9.1.2 Critical loads in tonf obtained using shell elements*

| Case number | | 1 | 2 | 3 | 4 |
|---|---|---|---|---|---|
| Reference | | 0.5712 | 0.1428 | 2.2846 | 1.1684 |
| Element type | Number of elements | | | | |
| Tria-3 | 30 | 0.5739 | 0.1430 | 2.3293 | 1.1804 |
| Quad-4 | 15 | 0.5736 | 0.1429 | 2.3245 | 1.1790 |
| Tria-6 | 30 | 0.5698 | 0.1427 | 2.2628 | 1.1621 |
| Quad-8 | 15 | 0.5705 | 0.1428 | 2.2749 | 1.1656 |

*Table 9.1.3 Critical loads in tonf obtained using solid elements*

| Case number | | 1 | 2 | 3 | 4 |
|---|---|---|---|---|---|
| Reference | | 0.5712 | 0.1428 | 2.2846 | 1.1684 |
| Element type | Number of elements | | | | |
| Hexa-8 | 15 | 0.5747 | 0.1430 | 2.3421 | 1.1841 |
| Tetra-10 | 90 | 0.5725 | 0.1429 | 2.3065 | 1.1747 |
| Penta-15 | 40 | 0.5711 | 0.1428 | 2.2835 | 1.1681 |
| Hexa-20 | 15 | 0.5710 | 0.1428 | 2.2827 | 1.1678 |

# 9.2 Three member frame

| | |
|---|---|
| **REFERENCE** | Timoshenko et al.[2] |
| **ELEMENTS** | Bar elements |
| **MODEL FILENAME** | Buckling02.fea |

Figure 9.2.1 shows a plane frame structure subjected to two vertical point forces. The buckling load is determined for different cases in which different numbers of elements per member are considered. In Figure 9.2.2, the typical buckling mode is depicted.

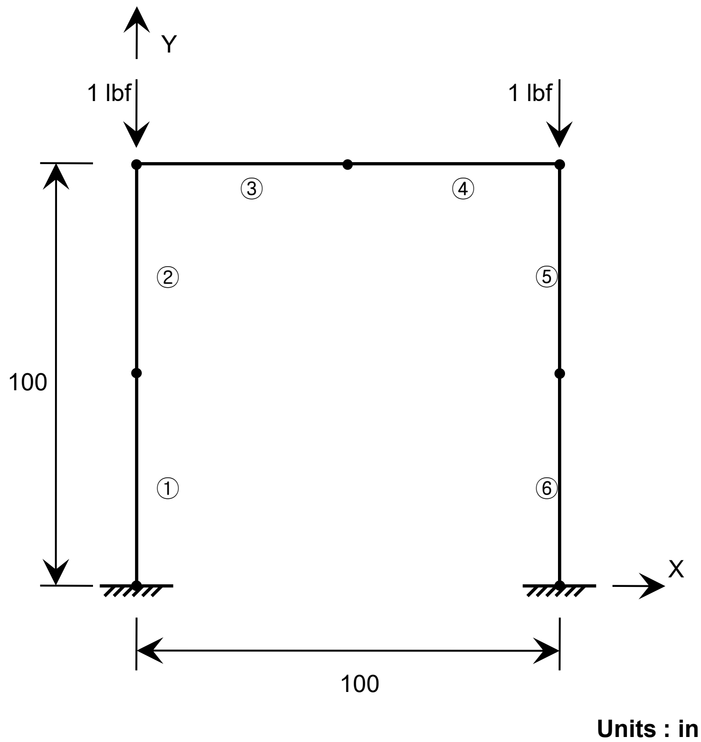


Figure 9.2.1
Three-member frame model

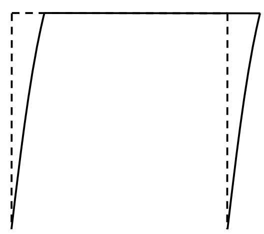

Figure 9.2.2
Buckling mode shape

| | | |
|---|---|---|
| **Material data** | Conductivity | $E = 1 \times 10^6$ psi |
| **Section property** | Area | $A = 1.0\ in^2$ |
| | Moment of inertia | $I = 1.0\ in^4$ |

*Table 9.2.1 Critical loads in lbf obtained using bar elements*

| Reference | | *737.9* |
|---|---|---|
| Element type | Number of elements | |
| Bar-2 | 2 per member | *739.8* |
| | 4 per member | *737.6* |
| | 8 per member | *737.5* |

# 9.3 Uniaxially compressed clamped square plate

| | |
|---|---|
| **REFERENCE** | Chajes[3] |
| **ELEMENTS** | Shell elements, Solid elements |
| **MODEL FILENAME** | Buckling03.fea |

Figure 9.3.1 shows a square plate subjected to a compressive load. The linear buckling analysis is carried out to determine the critical load with a clamped boundary condition. One quarter model is used due to the symmetric boundary condition.

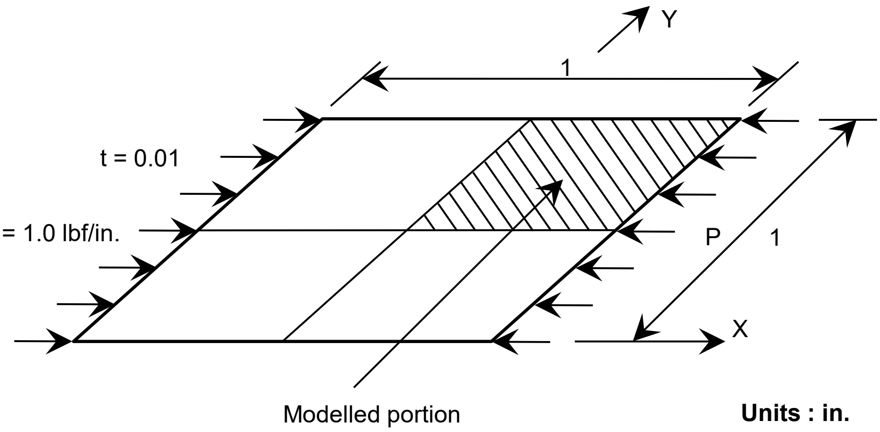


Figure 9.3.1
Clamped square plate model

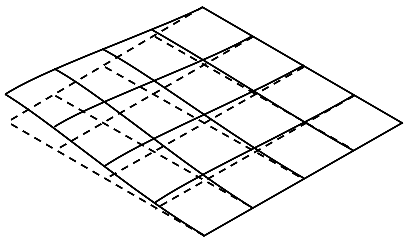

Figure 9.3.2
Buckling mode shape

| | | |
|---|---|---|
| **Material data** | Young's modulus | E = 11.064 $\times$ 10$^5$ psi |
| | Poisson's ratio | $\nu$ = 0.3 |
| **Section property** | Thickness | t = 0.01 in |

*Table 9.3.1 Critical distributed load in lbf. Obtained using shell elements*

| Reference | | *100.7* |
|---|---|---|
| Element type | Number of elements | |
| Tria-3 | 32 | *111.7* |
| Quad-4 | 16 | *107.3* |
| Tria-6 | 32 | *97.2* |
| Quad-8 | 16 | *100.6* |

*Table 9.3.2 Critical distributed load in lbf. Obtained using solid elements*

| Reference | | *100.7* |
|---|---|---|
| Element type | Number of elements | |
| Hexa-8 | 16 | *98.0* |
| Penta-15 | 32 | *127.8* |
| Hexa-20 | 16 | *111.8* |

# 9.4 Rectangular plate under concentrated center load

| | |
|---|---|
| **REFERENCE** | Timoshenko et al.[2] |
| **ELEMENTS** | Shell elements |
| **MODEL FILENAME** | Buckling04.fea |

Figure 9.4.1 shows a rectangular plate subjected to a point force. All the sides are simply supported, and the edge AD is constrained in the Y direction. A concentrated force is applied at the center of BC (point E). The linear buckling analysis is carried out to obtain the lowest critical load.

Figure 9.4.1
Simply supported rectangular plate model

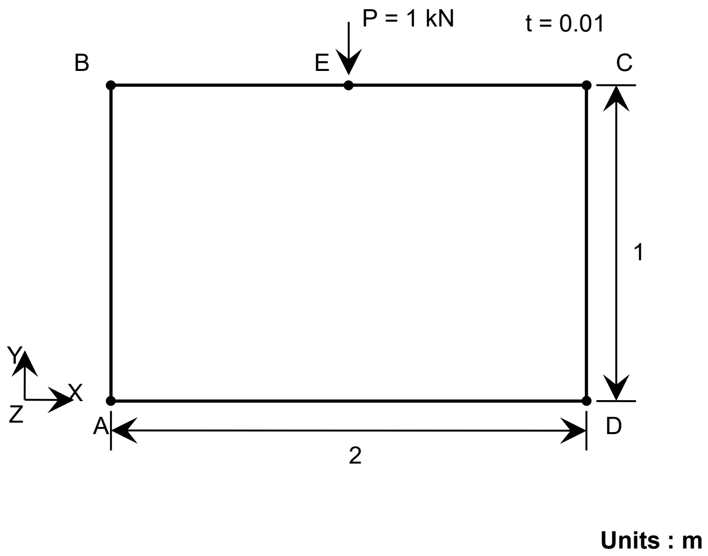


| | | |
|---|---|---|
| **Material data** | Young's modulus | E = 200 GPa |
| | Poisson's ratio | $\nu$ = 0.3 |
| **Section property** | Thickness | t = 0.01 m |

*Table 9.4.1 Critical load in kN obtained using shell elements*

| Reference | | *330* |
|---|---|---|
| Element type | Number of elements | |
| Tria-3 | 144 | *342* |
| Quad-4 | 72 | *327* |
| Tria-6 | 36 | *316* |
| Quad-8 | 18 | *320* |

*Table 9.4.2 Critical load in kN obtained using solid elements*

| Reference | | *330* |
|---|---|---|
| Element type | Number of elements | |
| Hexa-8 | 72 | *298* |
| Penta-15 | 36 | *377* |
| Hexa-20 | 18 | *330* |

# 9.5 Axially compressed cylinder

| | |
|---|---|
| **REFERENCE** | Simo et al.[4] |
| **ELEMENTS** | Shell elements, Solid elements |
| **MODEL FILENAME** | Buckling05.fea |

Figure 9.5.1 shows a cylindrical shell model subjected to a distributed compressive load. Both ends of the cylinder are clamped in the transverse direction. One eighth portion of the cylinder is modeled with a symmetric boundary condition. The linear buckling analysis is carried out to determine the lowest critical load factor. The typical mode shape is depicted in Figure 9.5.2.

Figure 9.5.1
Axially compressed cylinder model

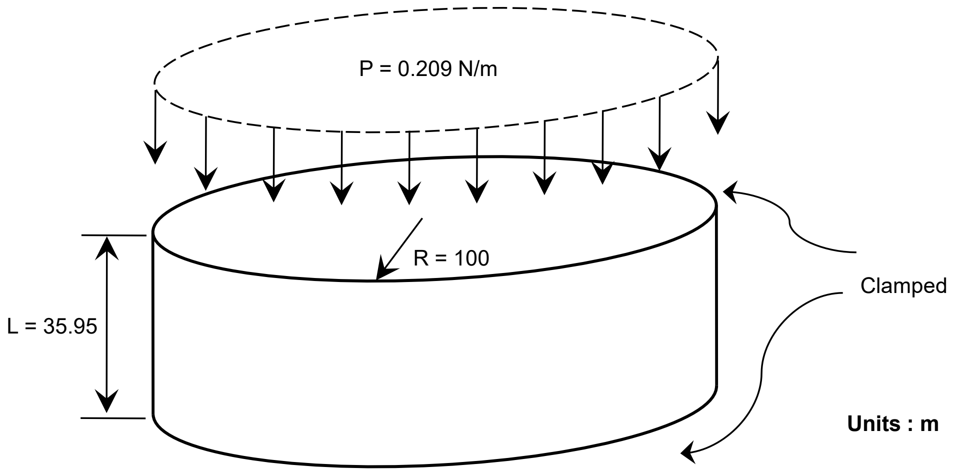


Figure 9.5.2
Buckling mode shape

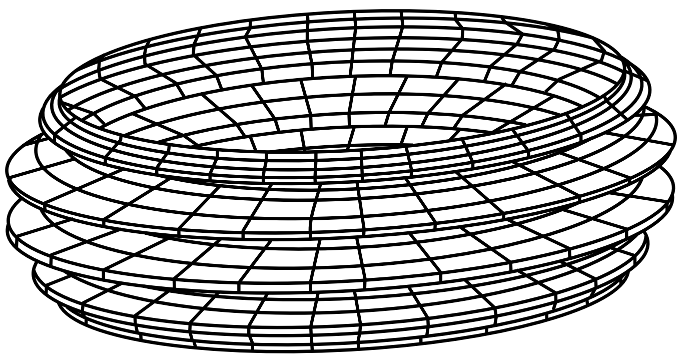

| | | |
|---|---|---|
| **Material data** | Young’s modulus | E = 567 Pa |
| | Poisson’s ratio | $\nu$ = 0.3 |
| **Section property** | Thickness | t = 0.247 m |

*Table 9.5.1 Critical load factor obtained using shell elements*

| Reference | | *1.0833* |
|---|---|---|
| Element type | Number of elements | |
| Tria-3 | 840 | *1.1129* |
| Quad-4 | 420 | *1.1370* |
| Tria-6 | 840 | *1.0123* |
| Quad-8 | 420 | *1.0148* |

*Table 9.5.2 Critical load factor obtained using solid elements*

| Reference | | *1.0833* |
|---|---|---|
| Element type | Number of elements | |
| Hexa-8 | 420 | *1.0630* |
| Hexa-20 | 420 | *0.9950* |

# 9.6 L-bracket plate under in-plane load

| | |
|---|---|
| **REFERENCE** | Simo et al.[4] and Argyris et al.[5] |
| **ELEMENTS** | Shell elements, Solid elements |
| **MODEL FILENAME** | Buckling06.fea |

Figure 9.6.1 shows a clamped L-shape plate subjected to an in-plane bending load. Linear buckling analysis is performed to obtain the critical load. The critical load induces lateral buckling of which the mode shape is depicted in Figure 9.6.2.

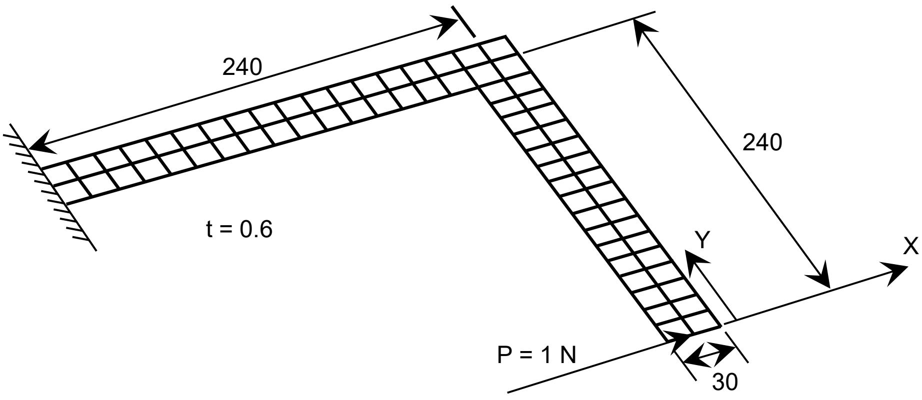


Figure 9.6.1
L-bracket plate model

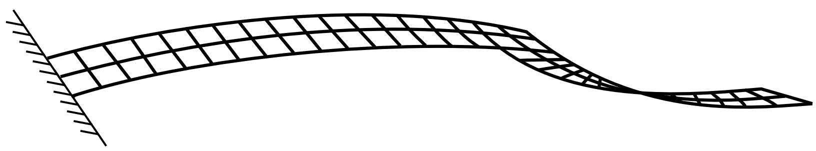

Figure 9.6.2
Buckling mode shape

| | | |
|---|---|---|
| **Material data** | Young's modulus | E = 71.240 GPa |
| | Poisson's ratio | $\nu$ = 0.3 |
| **Section property** | Thickness | t = 0.6 mm |

*Table 9.6.1 Critical load in N obtained using shell elements*

| Reference | | *1.137 (Simo et al.) 1.155(Argyris et al.)* |
|---|---|---|
| Element type | Number of elements | |
| Tria-3 | 136 | *1.183* |
| Quad-4 | 68 | *1.199* |
| Tria-6 | 34 | *1.120* |
| Quad-8 | 17 | *1.189* |

*Table 9.6.2 Critical load in N obtained using solid elements*

| Reference | | *1.137 (Simo et al.) 1.155(Argyris et al.)* |
|---|---|---|
| Element type | Number of elements | |
| Hexa-8 | 68 | *1.198* |
| Penta-15 | 34 | *1.238* |
| Hexa-20 | 17 | *1.188* |

# References

1 J.M. Gere and S.P. Timoshenko, Mechanics of Materials, 2nd Edition, Thomson Brooks/Cole, California, New York, 1984

2 S.P. Timoshenko and J.M. Gere, Theory of Elastic Stability, 2nd Edition, McGraw-Hill, New York, 1961

3 A. Chajes, Principles of Structural Stability Theory, Prentice-Hall, Englewood Cliffs, N.J,1974

4 J.C. Simo, D.D. Fox and M.S. Rifai, “On a Stress Resultant Geometrically Exact Shell Model. Part III: The Computational Aspects of the Nonlinear Theory,” Computer Methods in Applied Mechanics and Engineering, Vol. 79, pp. 21-70, 1990

5 J.H. Argyris, H. Balmer, J.St. Doltsinis, P.C. Dunne, M. Haase, M. Hasse, M. Kleiber, G.A. Malejannakis, H.P. Mlejenek, M. Muller and D.W. Scharpf, “Finite Element Method – The natural approach,” Computer Methods in Applied Mechanics and Engineering, Vol. 17/18, pp. 1-106, 1979